

Environmental Science Water Research & Technology

Accepted Manuscript

This article can be cited before page numbers have been issued, to do this please use: S. Islam, S. Das, G. Mishra, B. Das, A. Malakar, I. Carlomagno, C. Meneghini, G. de Giudici, L. P. L. Gonçalves, J. P. S. Sousa, Y. V. Kolen'ko, A. C. Kuncser and S. Ray, *Environ. Sci.: Water Res. Technol.*, 2020, DOI: 10.1039/D0EW00357C.



This is an Accepted Manuscript, which has been through the Royal Society of Chemistry peer review process and has been accepted for publication.

Accepted Manuscripts are published online shortly after acceptance, before technical editing, formatting and proof reading. Using this free service, authors can make their results available to the community, in citable form, before we publish the edited article. We will replace this Accepted Manuscript with the edited and formatted Advance Article as soon as it is available.

You can find more information about Accepted Manuscripts in the [Information for Authors](#).

Please note that technical editing may introduce minor changes to the text and/or graphics, which may alter content. The journal's standard [Terms & Conditions](#) and the [Ethical guidelines](#) still apply. In no event shall the Royal Society of Chemistry be held responsible for any errors or omissions in this Accepted Manuscript or any consequences arising from the use of any information it contains.

Ferrihydrite, a natural nanocrystal of iron, can adsorb and consequently eliminate contaminant ions when taken out of water at specific point-of-zero-charge. We propose to extract ferrihydrite clusters are wide range of pH and iron concentrations using zinc acetate coagulant. Added zinc is also removed due to strong chemical interaction between Fe and Zn leaving water free from both zinc and iron.

ARTICLE

Coagulating and flocculating Ferrihydrite: Application of Zinc Acetate salt

Samirul Islam^a, Sanjit Das^a, Geetanjali Mishra^a, Bidisa Das^{b,c}, Arindam Malakar^a, Ilaria Carlomagno^d, Carlo Meneghini^d, Giovanni De Giudici^e, Liliana P. L. Gonçalves^f, Juliana P. S. Sousa^f, Yuri V. Kolen'ko^f, Andrei Cristian Kuncser^g, and Sugata Ray^{a,c,*}

Received 00th January 20xx,
Accepted 00th January 20xx

DOI: 10.1039/x0xx00000x

This paper outlines a method of extraction of iron from water in form of iron oxyhydroxide natural nanoclusters at comparatively low concentrations and varied ranges of pH using zinc acetate salt. The zinc acetate salt dissociates into Zn^{2+} and acetate ions in water where Zn^{2+} interacts with the iron clusters present in a solution of given iron concentration and pH, while acetate ion helps in charge-neutralization based coagulation and consequent precipitation of such nanoclusters. The Zn^{2+} ions may also lead to the growth of layered zinc hydroxide (LZH) nanosurfaces at $\text{pH} \geq 6$ at sufficient loading. The advantage of this method is the active chemical interaction of Zn^{2+} with Fe clusters, followed by growth, which ensures that only a part of the added Zn remains in the water while the rest precipitates out along with the residual iron oxyhydroxide, especially at higher pH. The solid precipitated under various different conditions, were successfully evaluated by XRD (formation of ferrihydrite-like nanoclusters (n-Fh)), FTIR (presence of acetate in the solid n-Fh), TEM (presence of zinc at higher pH), EXAFS (local structural characterization). ICP analysis of the obtained solid and the corresponding filtrate revealed the removal efficiency of iron and zinc from the solution under various initial concentrations and pH. This method of extracting soluble Fh-like nanoclusters by charge neutralization appears to be a suitable promising tool for water purification, because ferrihydrite is capable of isolating other adsorbed contaminants from water, along with itself.

Introduction

Particles of colloidal or lesser dimensions are able to retain a dissolved state because of their stability in the solution i.e. the capacity of such particles to remain as independent entities within a dispersion. All particles in a liquid medium possess several different interfacial phenomena which include the effects of the surface charge carried by particles and the degree of hydration (or solvation) of the particles' surface layers. Due to the presence of similar charge at the surface of each particle, the particles tend to repel each other which is the main reason behind the dispersion, denying aggregation, and thereby creating colloidal suspensions.¹ The process of destabilization of such dispersed contaminants goes through coagulation and

flocculation. Different mechanisms of coagulation using chemical agents include double layer compression, charge neutralization, sweep coagulation, and interparticle bridging.^{1,2} Among these, charge neutralization and sweep coagulation (or sweep flocculation) are the two most useful ones. The most common coagulants, that are used in these processes in real life to clean turbid water, are Alum, Ferric Chloride, and Ferric Sulphate.^{3,4}

It is known that particulate contaminants responsible for turbidity of water are typically negatively charged and therefore, common coagulants are chosen in such a way that they form positively charged species in water upon hydrolysis. For example, iron-based coagulants produce iron oxyhydroxide clusters in water having positive surface charge which are capable of interacting with particulate matters through Coulombic attraction. Therefore, the mechanism of coagulation involves either the adsorption of coagulant species to the contaminant or the entrapment of the contaminant within a large volume of hydroxide precipitate, originating from the coagulant, both operating via Coulombic attraction. One of the main characteristics of coagulants suitable for practical separation of contaminants has to be that it should neither alter the pH of solution nor it should add any significant amount of residual element/ion to the system. For example, most prominent Fe and Al- coagulants always get rid of Fe and/or Al by precipitating corresponding hydroxides.

^a School of Materials Science, Indian Association for the Cultivation of Science, Jadavpur, Kolkata 700032, India

^b School of Applied and Interdisciplinary Sciences, Indian Association for the Cultivation of Science, Jadavpur, Kolkata 700032, India.

^c Technical Research Centre, Indian Association for the Cultivation of Science, Jadavpur, Kolkata 700032, India

^d Dipartimento di Scienze, Università Roma Tre, Via della Vasca Navale, 84 I-00146 Roma, Italy

^e Department of Chemical and Geological Sciences, University of Cagliari, via Trentino 51, I-09127 Cagliari, Italy.

^f International Iberian Nanotechnology Laboratory, Av. Mestre José Veiga s/n, 4715-330 Braga, Portugal

^g National Institute of Materials Physics, Laboratory of Atomic Structures and Defects in Advanced Materials, Atomistilor 105 bis, 077125 Magurele, Romania

*Correspondence to: mssr@iacs.res.in.

Electronic Supplementary Information (ESI) available: [details of any supplementary information available should be included here]. See DOI: 10.1039/x0xx00000x

Clearly, nanoclusters of iron oxyhydroxide or ferrihydrite (Fh)^{5,6} already existing in iron-contaminated water cannot be extracted using ferric or aluminium coagulants because of the same positive surface charge in both the coagulator and the contaminant. In the present manuscript we are proposing a novel method of extracting these clusters using zinc acetate as the coagulating agent. However, it is important to note here that the structure of iron nanoclusters is not rigid and therefore, we are refraining from strictly naming the whole class of the clusters as ferrihydrite, rather we identify them as ferrihydrite class of systems, having similar structural motifs (n-Fh). In any case, this n-Fh continues to exist as colloidal clusters and do not precipitate out of the solution until the pH of the solution goes up to 7-9, which is the point-of-zero charge (PZC) of n-Fh at the initial iron concentration range of 0.1-20 mg/L.⁷⁻¹² Interestingly, n-Fh is known to be an excellent adsorbent which captivates other more toxic ions and therefore, methods of removing these n-Fh clusters around neutral pH and low Fe concentration could be of excellent use in the context of decontamination of water. This present attempt of extracting the n-Fh clusters at different pH and Fe concentrations can be considered to be a step towards that goal.

Understandably, one needs to apply specific negatively charged coagulating agents here so that the positive charges of n-Fh nanoclusters are effectively neutralized in the pH range of interest, while cationic component of the coagulator is also removed by certain inherent chemical reaction and growth mechanism. In this context, zinc-based compounds could be most suitable because zinc toxicity is low and very active chemical interaction between zinc and hydrous ferric oxide/ferrihydrite/goethite in aqueous medium at different pH and loading concentrations are already known in the literature.¹³⁻¹⁸ According to the literature, at low pH and low Zn/Fe ratio, octahedral zinc hexahydrate gets transformed to a tetrahedrally coordinated moiety and form bidentate mononuclear inner sphere complex.^{13, 14} However, the situation changes with increase in pH and Zn loading, where Zn(II) ions begin to form corner-sharing polynuclear complexes on the surface of ferrihydrite which acts as the precursor of layered zinc hydroxide structure.¹⁴ These layered zinc hydroxides (LZH) are quite stable and can precipitate out of water at pH ≥ 6 .¹⁹⁻²¹ It is observed experimentally that zinc loading on n-Fh clusters (sorbate/sorbent \Rightarrow $\text{Zn(M)}_{\text{adsorbed}} / [\text{Zn(M)}_{\text{adsorbed}} + \text{Fe(M)}_{\text{residue}}]$) is quite significant in almost the full pH range and at various initial Fe concentrations, which ensures removal of the same along with precipitated n-Fh residues. Of course, the precipitation of target n-Fh clusters itself is triggered by the acetate ions through charge neutralization, followed by flocculation. It is also interesting to note that the layered zinc hydroxide structure itself has a negative zeta potential till pH 8 and can also act as possible coagulating agent for positively charged n-Fh clusters.

Naturally, the proposed method can significantly help the water decontamination technology because in this way toxic species, adsorbed on ferrihydrite-like surface, also can get removed from water.

Experimental

Materials

In the experiment, Zinc acetate dihydrate (Sigma, 98%) was used as coagulant. Iron (III) chloride (Sigma, >99%), KOH (Chem Labs, 85%) and Suprapure HNO₃ (Merck, Germany, 65%) were used to prepare all the solutions of different pH and concentrations. Deionized water (resistivity 18.2 M Ω -cm) used for solutions was obtained from a Millipore filter system. All the chemicals used were of analytical reagent grade and were used without any further purification.

Synthesis methods

Primarily, solutions of three different ranges of concentrations of Fe were prepared in our laboratory;

- Concentrated Fe solutions (~200 mg/L; equivalent to acid mine drainage; marked as CF);
- Mid-range of Fe concentrations (~50 mg/L; equivalent to normal waste water; marked as F);
- Fe concentration nearly equivalent to natural groundwater condition (50 - 200 $\mu\text{g/L}$; equivalent to groundwater samples indicated as DF).

Next, all these solutions have been treated with a certain amount (20 mg/L - 100 mg/L) of zinc acetate salt under continuous stirring or simple shaking at ambient condition, and the precipitate has been filtered out using a Whatmann 42 filter paper. The precipitation time varied based on concentration and pH. It is important to mention here that the minimum required amount of zinc acetate naturally depends critically on the concentration of Fe and the corresponding pH of the solution. This is shown as a contour plot in Fig. 1(a), which depicts that the maximum quantity of zinc acetate is required for precipitation of n-Fh from very low concentration, highly acidic (low pH) solutions of Fe, and this requisite amount progressively got reduced either with increasing Fe concentration or increasing pH of the solution. However, no precipitation was observed in solutions of concentration below 400 mg/L of iron at pH 3.5 or below. The red part of the contour plot indicates these regions where we failed to trigger precipitation of n-Fh even after addition of very large quantities of Zn(Ac)₂ and waiting for significant no. of days. Highly concentrated solutions (CF) have been used for the collection of sufficient residue for further detailed structural (XRD, XAFS), chemical, and morphological (TEM) analysis as well as for having clearer and visible results (see video presented in Supplementary Materials).

Characterizations

X-ray diffraction (XRD) patterns of the obtained solids were investigated in the MCX beamline of Elettra synchrotron centre, Italy. The ultrahigh-resolution transmission electron microscopy (TEM) (JEOL-JEM 2100F) were carried out along with HRTEM (at Bucharest National Institute of Materials Physics) for chemical and morphological information. Fourier

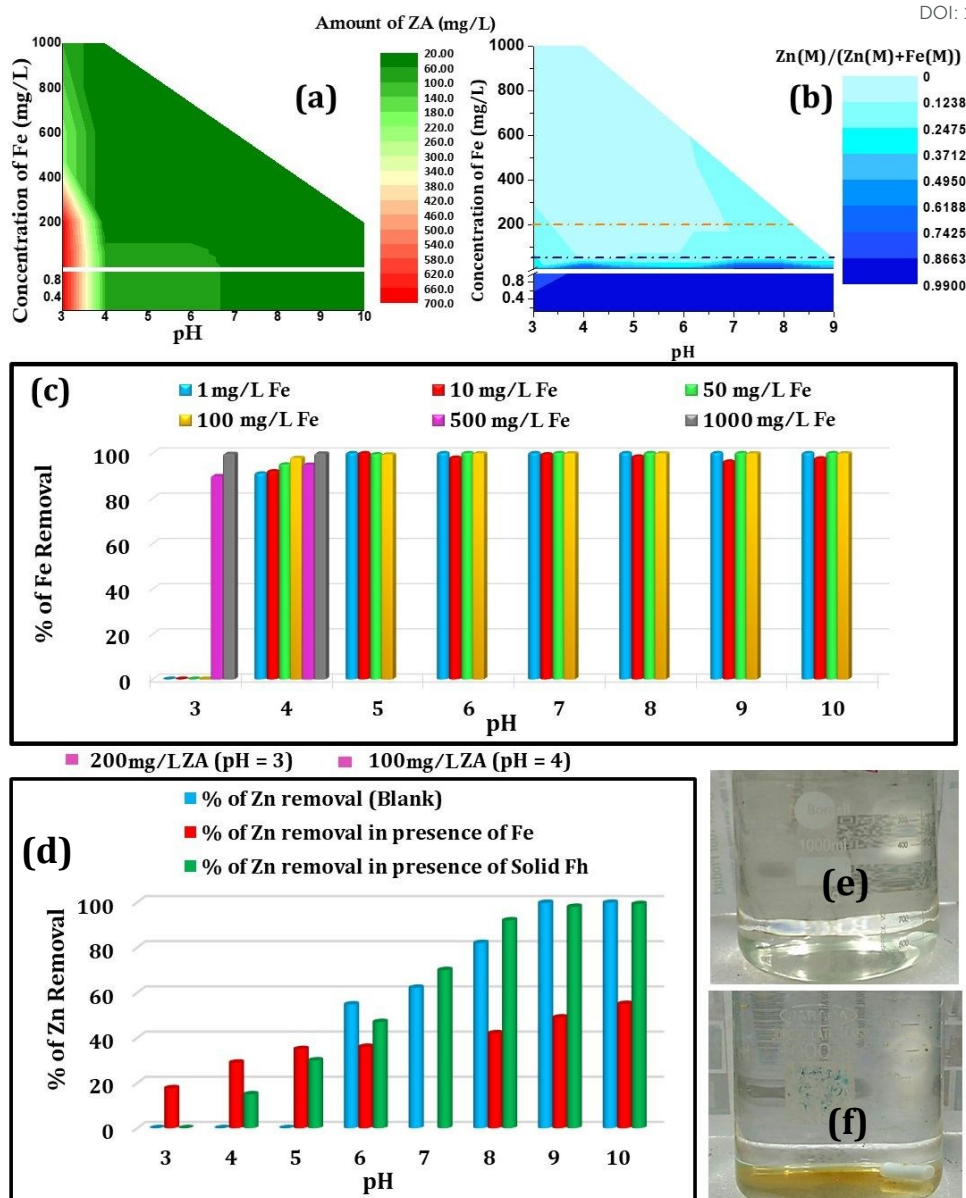


Figure 1: (a) A contour plot of initial concentration of Fe as a function of pH where the colour coding indicates that amount of zinc acetate required for precipitation, (b) same as (a) but the colour coding indicates the zinc loading i.e. the amount of zinc that got attached to the precipitated solid, (c) % of Fe³⁺ and (d) % of Zn removal at different concentrations and pH; (e) and (f) Photographs of 1 mg/L Fe³⁺ solution (pH 7) showing clear solution in absence of zinc acetate while precipitate with zinc acetate, respectively.

Transform Infrared (FTIR) spectra of the obtained solid were recorded in the wave number range of 400–4000 cm⁻¹ in a FTIR spectrophotometer (Perkin Elmer India Pvt. Ltd., SPECTRUM 100) with scanning resolution of 4 cm⁻¹ using KBr as a reference. The chemical analysis of the water samples, both before and after treatment and of the residue were carried out by ICP-OES (Perkin-Elmer Optima 2100 DV). The local structure of the solid was probed by X-ray absorption fine structure (XAFS) spectroscopy at the Fe K-edge collected at the XAFS beamline (Elettra Synchrotron Center, Italy). Fitting of the extended (EXAFS) signal was carried out within a multi-shell data fitting

procedure using the local atomic cluster derived from density functional theory (DFT) as a model for Fe average local structure.

Theoretical Methods

The electronic structure studies for the relevant reference cluster of n-Fh and related species were performed using DFT as implemented in the Gaussian 09 suite of programs.²² Studies were performed using the B3LYP 6-8 hybrid functional with the 6-31G** basis sets for all atoms. The stable clusters were determined by full geometry optimization in the gas-phase

which were then confirmed to be the stable minimum on the potential energy surface by harmonic frequency calculations.

Results and Discussion

Chemical Analyses

Simple addition of a requisite quantity of zinc acetate salt in aqueous iron solutions at various pH and concentrations followed by constant stirring results immediate precipitation of n-Fh clusters. However, the situation changed below pH = 3.5 as no solid precipitated from solutions containing Fe upto 400 mg/L, while precipitation did occur for more concentrated solutions but over a longer period of time. The required amount of zinc acetate used for different concentrations of Fe solutions and at different pH has been represented as a contour plot in Fig. 1 (a). The red part indicates the condition where no precipitation occurred (discussed above) even after the addition of very large amount of zinc acetate. In the pH range of 4-7, for solutions having concentration of Fe nearly equivalent to groundwater to 100 mg/L, the amount of zinc acetate utilized to coagulate the unstable clusters is 100 mg/L, whereas for higher concentration of Fe, the required amount of zinc acetate got reduced for the same pH ranges. As a result, the zinc loading ($Zn(M)/[Zn(M)+Fe(M)]$ in the residue) varied widely, as is shown in another contour plot in Fig. 1(b). This figure should be analysed with respect to the results presented in refs. 13 and 14, where however, the Fe-Zn interaction in aqueous medium has been probed under two particular conditions, slightly different from ours. In one, Fe and Zn coexist from the beginning while pH is progressively taken to the desired value or until coprecipitation occurs. In another, solid ferrihydrite is grown separately and the growth of zinc moieties on the ferrihydrite bed via adsorption-growth mechanism is studied. In our case, as more emphasis has been given to create a practical application by extracting n-Fh from aqueous solutions of different Fe concentrations and pH, we always allowed unhindered growth of such Fe clusters at a given concentration and target pH and only at the end added zinc acetate so that the growth of the iron clusters is in no way affected by surrounding pre-added Zn^{2+} ions. However, still a comparison of the proposed results with that presented in refs. 13 and 14 provide important clues which help to comprehend our observations.

It has been shown in refs. 13 and 14 that below pH = 6.5, $Zn(II)$ ions form corner-sharing, mononuclear, bidentate inner-sphere complexes with ferrihydrite for all loading. However, at pH ≥ 6.5 and with a $Zn(II)$ loading of ≥ 0.1 , Zn starts to form polynuclear complexes which finally nucleates layered zinc hydroxide structure. Here Fig. 1(b) clearly shows that in this case, for pH ≥ 6.5 , the zinc loading is invariably higher than 0.1 for all initial Fe concentrations. However, the loading remains very high (> 0.25) for Fe solutions of concentration upto 35 mg/L and it is expected that LZH precipitates out along with n-Fh in these cases.^{13,14} Interestingly, the loading remains high even below pH = 6.5 for solutions of concentration 35 mg/L or below, ensuring Zn removal to a large extent, albeit in a possible different form.

The situation changes for lower pH and Fe concentrations ≥ 50 mg/L. The attachment of Zn to the n-Fh cluster reduces in these cases (Zn loading ≤ 0.125) as the starting Zn/Fe ratio itself was less, but even then at least 20% Zn gets removed at pH = 3 for a 50 mg/L Fe solution, unlike the case of Zn interaction with the ferrihydrite bed (Fig. 1(d)). In Fig. 1(d) we show the percentage of Zn removal at different pH for a 50 mg/L Fe solution (the blue dot-dash line in Fig. 1(b)), in order to compare the proposed method with the process described in ref. 14. Clearly in our method for a 50 mg/L iron solution, the Zn loading always remains between 0.125 to 0.25 throughout the pH range, ensuring quite significant zinc removal. The Zn loading for solutions below 400 mg/L Fe (red region in Fig. 1(a)) is obtained by estimating the removal of Fe and Zn from the solution after filtration, even though no visual precipitation occurred. Few interesting observations should be noted in the context of zinc loading under different conditions (Fig. 1(d)). For a blank 100 mg/L zinc acetate solution, precipitation starts to appear only at pH = 6 which is the onset of LZH formation, as has been shown by previous literature.¹⁹⁻²¹ However, in presence of a ferrihydrite bed, the zinc removal more or less follows the blank experiment but as an exception, zinc starts to get removed from pH = 4 itself which indicates chemical attachment of Zn to the ferrihydrite surface at lower pH. Interestingly, the situation changed even further in this case where the zinc removal profile follows a different trend throughout. In this case, zinc starts to get removed from pH = 3 itself and to a larger extent than the ferrihydrite bed till pH = 6, but unlike the blank or the ferrihydrite bed, it falls short of nearly complete removal even at pH = 10. Qualitatively, through these representative experiments with 50 mg/L iron solution, it can be easily concluded that the nature of Zn-Fe interaction differed in the proposed case quite significantly but most importantly, there is substantial zinc removal in our process throughout the pH range. However, from an applicational point of view, it is important to note here that the iron removal has always remained close to 100% for every concentration between 1 to 1000 mg/L and at every pH between 3 to 10 (Fig. 1(c)). Therefore, zinc acetate appears to work as an extremely efficient coagulant for n-Fh with immediate precipitation, which

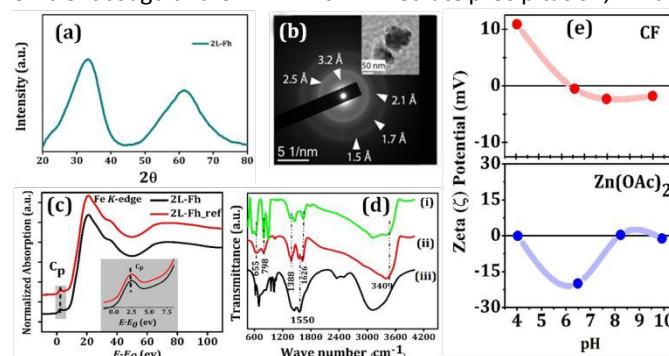


Figure 2: (a) XRD patterns from 2L-Fh; (b) SAED patterns from 2L-Fh, corresponding low resolution TEM image are shown in the inset; (c) Fe K-edge XANES spectrum from 2L-Fh ref and 2L-Fh solid; (d) FTIR spectra of (i) Fh clusters without zinc acetate, (ii) Fh clusters with zinc acetate, (iii) pure zinc acetate, respectively; (e) Zeta (ξ)-potential vs. pH of concentrated Fe and zinc acetate solutions, respectively.

is effective for a wide range of pH and concentration (clear solution of 1 mg/L Fe (pH~7) in absence of zinc acetate and with observable precipitates in presence of zinc acetate are shown in Fig. 1(e) and (f), respectively).

Structural Analyses

In order to confirm that the residue is indeed ferrihydrite-like and acetate is indeed accompanying it, solid precipitates, collected from the concentrated iron (CF) solution at pH 5.8, were characterized using X-ray diffraction (XRD) and FTIR measurements. All these solids that have been probed by different tools have all been collected from iron solution of 200 mg/L at different pH (red dash-dot line in Fig. 1(b)). The point to be considered here that the zinc loading is rather low <0.125 in these solids till at least pH = 7 and goes upto 0.25 till highest pH.

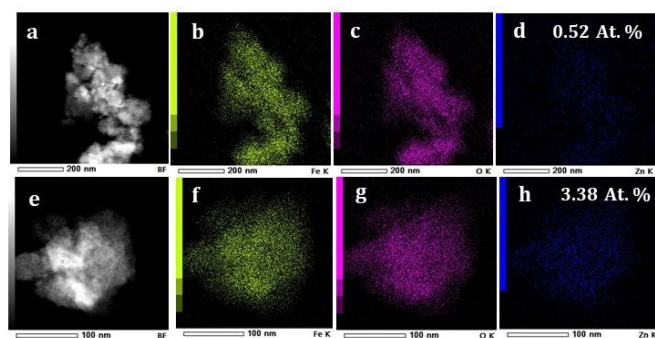


Figure 3: TEM image of the precipitate obtained at different pH; showing absence of Zn at pH = 4 (a, b, c, d) and presence of Zn at pH = 10 (e, f, g, h)

The two broad features observed in the XRD pattern (Fig. 2(a)) immediately lead to identification of 2-line ferrihydrite (2L-Fh) like phase formation. The selected area electron diffraction (SAED) image (Fig. 2(b)) further revealed the typical 2L-Fh like rings at 0.15 nm and 0.25 nm with shoulders at 0.17 nm, 0.21 nm, and 0.32 nm.^{23,24} Fig. 2(c) represents the Fe K-edge x-ray absorption near edge spectra (XANES) data from 2L-Fh like phase and a reference ferrihydrite sample 2L-Fh_{ref}. The Fe XANES spectra in all the cases appeared very similar, in particular the area A_p , and centroid C_p of the pre-edge peak (inset to Fig. 2(c) and Table S-1 of Supplementary Materials) indicate Fe(III) ions having average coordination around 5 which is consistent with the literature^{25,26} and DFT model cluster calculation (see later). Thorough details of the average local atomic structure around Fe ions are obtained from the analysis of the extended region (EXAFS) of the absorption spectra. The EXAFS experimental data and best fit curves are presented in Fig. S-2 of Supplementary Materials while the quantitative information of the local atomic structure is summarized in Table S1 which confirms very similar local atomic structure of Fe in these samples. The Fh structure is expected to have about 20% of tetrahedral and 80% of octahedrally coordinated Fe sites. Therefore, the average coordination number of around 5 depicts a large fraction of unsaturated bonds at the nanocluster surface or distorted FeO_6 octahedra in these samples. The Fe-O average distance of around 1.94 Å is consistent with $R_{\text{Fe-O}} = 1.93$ Å of Fig. S-2 (see Supplementary Materials). Noticeably the Fe-O₂ shell, observed weakly in synthetic 2L-Fh_{ref}, is absent in 2L-Fh, probably hindered by structural disorder, and/or due to

some local structure difference between Fh_{ref} and the obtained Fh-like precipitate. The Fe-Fe₁ shell around 3 Å and the Fe-Fe₃ around 3.4 Å of 2L-Fh_{ref} are consistently found in 2L-Fh sample. However, the weak intermediate Fe-Fe₂ shell goes missing in the analysis of the precipitate, pointing out some minor differences between the Fe local structures. Interestingly, the theoretical results also suggest a bimodal Fe-Fe distance distribution with two coordination shells in between 3-3.15 Å and 3.4-3.6 Å, roughly consistent with the experimental findings (see Supplementary Materials).

It is recently shown that a nearly spherical δ -Keggin ion cluster, $[\text{FeO}_4(\text{Fe}(\text{OH})_2(\text{H}_2\text{O}))_{12}]^{7+}$ is a potential building block for formation of n-Fh^{7,27} which has a central Fe^{3+} ion in tetrahedral environment and rest 12 peripheral Fe^{3+} ions exhibit two different types of octahedral co-ordinations.²¹ We analysed the optimized structure of δ -Keggin cluster in high-spin state and found the closest Fe-Fe distances are 2.98–3.05 Å. There is however, a set of longer non-bonded Fe-Fe distances found between the central tetrahedral Fe atom with the peripheral octahedral Fe atoms, which are 3.5–3.6 Å. The Fe-O distances in the central FeO_4 unit are ~1.90 Å, whereas Fe-O distances in case of the outer FeO_6 octahedra are 2.00–2.12 Å. We also find that the Fe-O(H) distances range from 1.90 to 1.98 Å whereas the Fe-O(H₂O) distances are longer, 2.12–2.20 Å, which surrounds the central tetrahedral Fe^{3+} . The size of the δ -Fe₁₃ cluster is ~7.5 Å without water molecules but appears ~11 Å if the co-ordinated water molecules are also considered. It is important to mention that the water molecules acting as ligands in neutral environment, may be exchanged with other suitable anions depending on the environment.

In order to confirm that the solid obtained as precipitate by the addition of zinc acetate contains acetate irrespective of pH and concentration of solution, FTIR analysis of the solid was carried out and provided in Fig. 2(d). In this figure, the sample was compared with pure zinc acetate as well as with that of the ferrihydrite sample obtained at PZC without addition of zinc acetate. In the solid, precipitated using zinc acetate, the bands at 1626 cm^{-1} (due to C=O group) and at 1550 cm^{-1} (due to strong asymmetric stretching band of carboxylate ion (COO^-)) signifies the presence of acetate ion in it, confirming the interaction of acetate with that of soluble Fh clusters to initiate the coagulation process. In this case, because of intramolecular hydrogen bonding in n-Fh clusters, frequency of C=O stretching reduces somehow as compared to pure zinc acetate. These extra bands are the signature of zinc acetate and are absent in the sample obtained by precipitating Fh clusters at PZC without zinc acetate. Apart from that other peaks, a peak at 1388 cm^{-1} is observed which appears due to carbonate ion (CO_3^{2-}) from air atmosphere. Peaks at 798 and 655 cm^{-1} (because of Fe-O stretching) are also observed which the fingerprint regions of M-O bindings are. So, from this observation, it can be concluded that the solid precipitate indeed contains acetate ion.

Next comes the important question of the role played by zinc acetate as an effective coagulant. In every sample, zinc acetate has been added to the solution after the solution pH has been brought to the required value (pH~3-10). So, it is expected that nucleation and optimum growth of Fh nanoclusters have already been achieved before zinc acetate is added to the solution.^{7,24,25,28-30} The results unambiguously show that addition of zinc acetate in these solutions helps the Fh nanoclusters to agglomerate and precipitate out. To further confirm this hypothesis, zeta potential vs. pH measurements of CF and zinc acetate solutions has been carried out and the results are summarized in Fig. 2(e). Clearly, the zeta potential of CF solution is positive at lower pH whereas it decreases continuously with increasing pH and crosses the zero line (PZC) at around neutral pH (Fig. 2(e)). On the other hand, the zinc acetate solution has more negative zeta potential within the pH range of 4-8 with a minima at around pH 6.5 while it remains nearly zero or slightly positive between pH 8 to 10 because of the formation of layered structure.

Hence, it is expected that suspended particles of Fh would be attracted by the suspended opposite charges (acetate anion and may even by LZH surface) by Coulombic interaction, especially in the pH range of 4 to 8. However, the method is expected to become less efficient between pH 6-7 because the value of the zeta potential becomes negative for both the Fe and Zn solutions which was quite clearly manifested in the time of triggering precipitation. Noticeably the precipitation time becomes particularly long in this pH range indicating reduced efficiency of the process.

It has been mentioned earlier that an useful coagulant should not add foreign ions/metals in the system and in this case we expected the Zn to be removed because of active chemical interaction between Zn and n-Fh clusters at all possible pH (Fig. 1(b)). The anticipated absence and presence of Zn metal in the precipitate at lower and higher pH (pH 4 and 10) respectively was verified by elemental mapping through TEM and shown in Fig. 3. At pH 4, there is little signature of Zn in the obtained precipitate (Fig. 3(d) which is consistent with low Zn loading below pH = 6 (Fig. 1(b)). With increasing pH up to 10, with enhanced Zn loading, Zn is clearly observed in the precipitate Fig. 3(h). It can be commented that the addition of Zn will be close to WHO permissible limit while decontaminating a solution of 1 mg/L Fe at pH~7.

Therefore, it is confirmed that addition of zinc acetate in aqueous iron solutions at various pH and concentrations followed by mechanical stirring, ensures the precipitation of 2L-Fh-like phase in each case without adding any extra significant contaminant or altering the pH, which is an important achievement in the field of water decontamination.

Conclusions

In summary, a simple method of extracting ferrihydrite clusters from water has been proposed in a wide range of pH and very

low iron concentrations. This has been achieved by addition of moderate amount of commercial zinc acetate salt which acts as an effective coagulant. Interestingly, the loading of zinc acetate as well as formation of LZH above pH = 6 ensure that the addition of zinc metal to the resultant water still remains limited. This finding can be implemented on water purification technology as these clusters are known to be excellent adsorbents which can chemisorb various types of inorganic contaminants, and therefore, easy withdrawal of the same immediately decontaminates water.

Conflicts of interest

There are no conflicts to declare.

Acknowledgements

S. R. thanks Department of Science and Technology (DST) [Project No. WTI/2K15/74] for funding, and for financial support by Indo-Italian Program of Cooperation for performing experiments at Elettra (Proposal No. 20160124, 20140355 and 20160124, CERIC 20167045), and Saha Institute of Nuclear Physics for carrying out experiments in Photon Factory. S. D. thanks the University Grants Commission (UGC) for fellowship. The Grant of Excellence Departments, MIUR (ARTICOLO 1, COMMI 314–337 LEGGE 232/2016), is gratefully acknowledged. Authors also thank A. C. Kuncser of the National Institute of Materials Physics, Laboratory of Atomic Structures and Defects in Advanced Material, (Romania) for TEM measurements.

Notes and references

1. Y. Zou, X. Wang, Y. Ai, Y. Liu, J. Li, Y. Ji and X. Wang, Coagulation Behavior of Graphene Oxide on Nanocrystalline Mg/Al Layered Double Hydroxides: Batch Experimental and Theoretical Calculation Study. *Environ. Sci. & Technol.*, 2016, **50**, 3658-3667.
2. B. Bolto and J. Gregory, Organic polyelectrolytes in water treatment. *Water Res.*, 2007, **41**, 2301-2324.
3. J. Bratby, Coagulation and Flocculation, Uplands Press LTD., England, 1980.
4. A. B. Dempsey, C. R. O'Melia, Removal of naturally occurring compounds by coagulation and sedimentation. *Critical Reviews in Environmental control*, 2009, **14**, 311-331.
5. J. L. Jambor and J. E. Dutrizac, Occurrence and constitution of natural and synthetic ferrihydrite, a widespread iron oxyhydroxide. *Chem. Rev.*, 1998, **98**(7), 2549-2585.
6. S. J. Smith, K. Page, H. Kim, B. J. Campbell, J. Borio-Goates, B. F. Woodfield, Novel synthesis and structural analysis of ferrihydrite. *Inorg. Chem.*, 2012, **51**, 6421-6424.
7. J. S. Weatherill, K. Morris, P. Bots, T. M. Stawski, A. Janssen, L. Abrahamsen, R. Blackham and S. Shaw, Ferrihydrite formation: The role of Fe₁₃ Keggin cluster. *Environ. Sci. Technol.*, 2016, **50**, 9333-9342.
8. U. Schwertmann, J. Friedl and H. Stanjek, From Fe(III) ions

- to ferrihydrite and then to hematite. *J. Colloid Interface Sci.*, 1999, **209**, 215-223.
9. U. Schwertmann, R. M. Cornell, Iron Oxides in the laboratory, 2nd ed., Wiley-VCH, Weinheim, 2000.
 10. R. M. Cornell, U. Schwertmann, The Iron Oxides: Structure, Properties, Reactions, Occurrences and Uses: Wiley-VCH: Weinheim, 2003.
 11. M. Zhu, C. Frandsen, A. F. Wallace, B. Legg, S. Khalid, H. Zhang, S. Mørup, J. F. Banfield and G. A. Waychunas, Precipitation pathways for ferrihydrite formation in acidic solutions. *Geochim. Cosmochim. Acta*, 2016, **172**, 247-264.
 12. L. Dyer, P. D. Fawell, O. M. G. Newman and W. R. Richmond, Synthesis and characterization of ferrihydrite/silica co-precipitates. *J. Colloid Interface Sci.*, 2010, **348**, 65-70.
 13. P. Trivedi, J. Dyer, D. L. Sparks, K. Pandya, Mechanistic and thermodynamic interpretations of zinc sorption onto ferrihydrite. *J. Colloid Interface Sci.*, 2004, **270**, 77-85.
 14. G. A. Waychunas, C. C. Fuller and J. A. Davis, Surface complexation and precipitate geometry for aqueous Zn(II) sorption on ferrihydrite I: X-ray absorption extended fine structure spectroscopy analysis. *Geochim. Cosmochim. Acta*, 2002, **66**, 1119-1137.
 15. P. Trivedi, L. Axe and T. A. Tyson, An analysis of zinc sorption to amorphous versus crystalline iron oxides using XAS. *J. Colloid Interface Sci.*, 2001, **244**, 230-238.
 16. P. A. O'Day, S. A. Carroll and G. A. Waychunas, Rock-water interactions controlling Zinc, Cadmium and Lead concentrations in surface waters and sediments, U. S. Tri-state mining district. 1. Molecular identification using X-ray absorption spectroscopy. *Environ. Sci. Technol.*, 1998, **32**, 943-955.
 17. P. Trivedi and L. Axe, Modelling Cd and Zn sorption to hydrous metal oxides. *Environ. Sci. Technol.* 2000, **34**, 2215-2223.
 18. N. Z. Misak, H. F. Ghoneimy and T. N. Morcos, Adsorption of Co²⁺ and Zn²⁺ ions on hydrous Fe(III), Sn(IV) and Fe(III)/Sn(IV) oxides: II. Thermal behaviour of loaded oxides, isotopic exchange equilibria and percentage adsorption-Ph curves. *J. Colloid Interface Sci.*, 1996, **184**, 31-43.
 19. B. Song, Y. Wang, X. Cui, Z. Kou, L. Si, W. Tian, C. Yi, T. Wei and Y. Sun, A series of unique architecture building of layered zinc hydroxides: Self-Assembling stepwise growth of layered zinc hydroxide carbonate and conversion into three-dimensional ZnO. *Cryst. Growth Des.* 2016, **16**, 887-894.
 20. A. Moezzi, A. McDonagh, A. Dowd and M. Cortie, Zinc hydroxyacetate and its transformation to nanocrystalline zinc oxide. *Inorg. Chem.*, 2013, **52**, 95-102.
 21. G. G. c. Arizaga, K. G. Satyanarayana and F. Wypych, Layered hydroxy salts: Synthesis, properties and potential applications. *Solid State Ionics*, 2007, **178**, 1143-1162.
 22. Gaussian 09, Revision C.01, M. J. Frisch, G. W. Trucks, H. B. Schlegel, G. E. Scuseria, M. A. Robb, J. R. J. Cheeseman, G. Scalmani, V. Barone, B. Mennucci, G. A. Petersson, H. Nakatsuji, M. Caricato, X. Li, H. P. Hratchian, A. F. Izmaylov, J. Bloino, G. Zheng, J. L. Sonnenberg, M. Hada, M. Ehara, K. Toyota, R. Fukuda, J. Hasegawa, M. Ishida, T. Nakajima, Y. Honda, O. Kitao, H. Nakai, T. Vreven, J. A. Montgomery, Jr. J. E. Peralta, F. Ogliaro, M. Bearpark, J. J. Heyd, E. Brothers, K. N. Kudin, V. N. Staroverov, T. Keith, R. Kobayashi, J. Normand, K. Raghavachari, A. Rendell, J. C. Burant, S. S. Iyengar, J. Tomasi, M. Cossi, N. Rega, J. M. Millam, M. Klene, J. E. Knox, J. B. Cross, V. Bakken, C. Adamo, J. R. Jaramillo, Gomperts, R. E. Stratmann, O. Yazyev, A. J. Austin, R. Cammi, C. Pomelli, J. W. Ochterski, R. L. Martin, K. Morokuma, V. G. Zakrzewski, G. A. Voth, P. Salvador, J. J. Dannenberg, S. Dapprich, A. D. Daniels, O. Farkas, J. B. Foresman, J. V. Ortiz, J. Cioslowski, and D. J. Fox, Inc. Gaussian, CT. Wallingford 2009.
 23. D. E. Janney, J. M. Cowley and P. R. Buseck, Transmission electron microscopy of synthetic 2- and 6-line ferrihydrite. *Clays Clay Miner.*, 2000, **48**, 111-119.
 24. F. M. Michel, L. Ehm, S. M. Antao, P. L. Lee, P. J. Chupas, G. Liu, D. R. Strongin, M. A. A. Schoonen, B. L. Phillips and J. B. Parise, The structure of ferrihydrite, a nanocrystalline material. *Science*, 2007, **316**, 1726-1728.
 25. M. Wilke, F. Farges, P. E. Petit, G. E. Brown and F. Martin, Oxidation state and coordination of Fe in minerals: An Fe K-XANES spectroscopic study. *American Mineralogist*, 2001, **86**, 714-730.
 26. F. Farges, Crystal chemistry of iron in natural grandidierites: an X-ray absorption fine structure spectroscopy study. *Phys. Chem. Min.*, 2001, **28**, 619-629.
 27. B. Das, Theoretical study of small iron-oxyhydroxide clusters and formation of ferrihydrite. *J. Phys. Chem. A*, 2018, **122**, 652-661.
 28. M. Zhu, C. Frandsen, A. F. Wallace, B. Legg, S. Khalid, H. Zhang, S. Mørup, J. F. Banfield and G. A. Waychunas, Precipitation pathways for ferrihydrite formation in acidic solutions. *Geochimica et Cosmochimica Acta*, 2016, **172**, 247-264.
 29. G. Ona-Nguema, G. Morin, F. Juillot, G. Calas and G. E. Brown, EXAFS analysis of arsenite adsorption onto two-line ferrihydrite, hematite, goethite and lepidocrocite. *Environ. Sci. Technol.* 2005, **39**, 9147-9155.
 30. Z. Li, T. Zhang and K. Li, One-step synthesis of mesoporous two-line ferrihydrite for effective elimination of arsenic contaminants from natural water. *Dalton Trans.* 2011, **40**, 2062-2066.

Zinc acetate salt is proposed as an effective coagulator for extracting ferrihydrite clusters from water, avoiding much Zn addition.

